Journal of Constructional Steel Research 138 (2017) 565–579

Contents lists available at ScienceDirect

Journal of Constructional Steel Research

Seismic risk assessment of cold-formed steel shear wall systems

Smail Kechidi [a,b], Luís Macedo [b], José Miguel Castro [b,*], Nouredine Bourahla [a]

[a] Geomaterials and Civil Engineering Laboratory, Department of Civil Engineering, Faculty of Technology, University of Blida 1, P.O. Box 270, Blida 09000, Algeria
[b] Faculty of Engineering, University of Porto, Rua Dr. Roberto Frias s/n, 4200-465 Porto, Portugal

ARTICLE INFO

Article history:
Received 10 April 2017
Received in revised form 1 August 2017
Accepted 6 August 2017
Available online 23 August 2017

Keywords:
Cold-formed steel shear wall systems
Steel moment frames
Probabilistic seismic performance assessment
Seismic risk

ABSTRACT

This paper presents the probabilistic seismic performance and risk assessment of cold-formed steel (CFS) sheathed shear wall panel (SWP) structures adopting conventional steel moment-resisting frame (MRF) systems as a benchmark with the aim of exploring the viability of using CFS-SWP as a new structural solution in seismic prone regions. A set of 12 building structures of both systems, with 2-, 4- and 5-storey, have been designed for two seismic intensity levels. To simulate their nonlinear behaviour, the structures were modelled adopting recently developed deteriorating hysteresis models. Based on probabilistic seismic hazard analyses (PSHA), a site-specific selection of ground motion records for Incremental Dynamic Analyses (IDA) has been carried out adopting the Conditional Mean Spectrum (CMS) as a more realistic target response spectrum. Subsequently, the seismic risk was evaluated over the structure lifetime (*i.e.*, 50 years) in terms of the annual probability of exceeding the Damage Limitation, No-Local Collapse and Near Collapse limit states. The importance and usefulness of the risk metrics are highlighted and adopted as an indicator to explore the behavioural features of both structural systems. Overall, the assessment procedure showed that both systems present an acceptable seismic performance and therefore the CFS-SWP can be seen as a reliable structural solution to achieve performance-based objectives in seismic regions.

1. Introduction

In constructional steel practice, conventional steel moment-resisting and concentrically-braced frames (MRFs and CBFs, respectively) represent the most common solutions for buildings to withstand lateral loads (wind and earthquake). The reliability of these lateral load resisting systems was confirmed and improved from the performance observed in past earthquake events and also from significant past research activities that have culminated in detailed seismic design provisions adopted worldwide. In recent years, new innovative systems to ensure high structural and environmental performance have emerged. Among others, cold-formed steel (CFS) shear wall panel (SWP), represents an effective structural system to resist lateral loads for low- and medium-rise CFS buildings, offering a potential benefit from using lightweight framing components, thus, limiting the seismic mass. Nevertheless, conventional steel MRFs and CBFs are still preferred due to the more complex analysis and design procedures required when dealing with thin-walled CFS framing members, which develop local instabilities and several failure mechanisms. Besides, the fact that there is no prescription in the European seismic code, Eurocode 8 (EC8) [1], for the design of CFS-SWP, hinders the use of this lateral load resisting system in construction practice.

A number of research activities on CFS have been carried out in North America by Branston et al. [2], Yu [3], Yu and Chen [4], Balh et al. [5], DaBreo et al. [6] and Liu et al. [7] through quasi-static tests on SWPs as well as a dynamic test program conducted by Shamim et al., [8]. Many experimental and numerical research activities were also undertaken in Europe with the aim of gaining a deep understanding of the behaviour of CFS components and broaden their use as a new structural solution. Landolfo et al. [9], Iuorio et al. [10] and Fiorino et al. [11] performed monotonic and cyclic tests on different configurations of sheathed SWPs and diagonal strap-braced walls. Fülöp and Dubina [12], Della Corte et al. [13] and Vincenzo et al. [14] conducted numerical and theoretical studies on sheathed SWPs and diagonal strap-braced walls. Fiorino et al. [15], Landolfo et al. [16], Fiorino et al. [17] and Fiorino et al. [18] proposed a seismic design method for 1-storey CFS buildings. Ultimately, the main outcomes of these studies served for the characterization of the monotonic and the cyclic nonlinear behaviour of CFS sheathed SWPs and diagonal strap-braced walls, and allowed to establish a design procedure of these structural components. It is noteworthy that all the above-described works addressed the sub-system level behaviour of the CFS lateral load resisting system. As far as the full structure behaviour is concerned, Peterman [19] has conducted shake table tests on two full-scale CFS framed 2-storey buildings. The results highlighted the adequate structural performance under seismic loads where the buildings showed to be stiffer and stronger than what they were designed for (sub-system level design).

* Corresponding author.
E-mail address: miguel.castro@fe.up.pt (J.M. Castro).

http://dx.doi.org/10.1016/j.jcsr.2017.08.011
0143-974X/

A subsequent numerical study performed by Leng [20] which addressed the advanced 3D modelling of 2-storey CFS buildings' structure adopting experimental data spanning from fastener to full scale shake table level tests. Based on fragility analyses, similar conclusions as extracted experimentally by Peterman [19] have been drawn regarding the structural performance where acceptable levels of collapse safety were achieved. Although a major understanding of the behaviour of CFS structures under seismic loading conditions has been learned, the potential of CFS systems has not been fully evaluated yet in terms of risk assessment, based on a probabilistic method incorporating uncertainties that arise from the occurrence and intensity of earthquakes for limit states probability of exceedance (PoE). Therefore, it is deemed necessary to incorporate much of the previous research findings into the context of structural reliability to identify the performance of CFS buildings in seismic regions lacking proper standardised specifications for seismic design and verification.

In this paper, a probabilistic framework for structural performance assessment of CFS-SWP system with reference to conventional steel MRFs in terms of seismic risk, is presented. For this purpose, 2-, 4- and 5-storey buildings of each structural system have been designed for two seismic intensity levels and then modelled using the OpenSees finite element (FE) software [21]. Incremental Dynamic Analyses (IDA) were performed to generate the required data for the development of fragility curves adopting the Conditional Mean Spectrum (CMS) [22] to select site-specific ground motion records. Subsequently, in order to provide insights into the relative performance of both structural systems, the seismic risk is evaluated over the structure lifetime (*i.e.*, 50 years) in terms of the annual probability of exceeding the Damage Limitation (DL), No-Local Collapse (NLC) and Near Collapse (NC) limit states following the probabilistic SAC/FEMA closed-form framework [23], assuming a biased hazard fitted with a second-order power-law function [24].

2. Seismic design provisions

2.1. Sheathed CFS-SWP system

The CFS-SWP using wood or steel sheathing boards is a code approved lateral load resisting system for low- and medium-rise CFS buildings in North America, Australia and New Zealand. It is composed of CFS C-shaped framing members (chord studs, studs and tracks as shown in Fig. 4a) attached to sheathing boards using screw fasteners. In addition to gravity load resistance, this structural system dissipates energy by taking advantage of the inelastic behaviour that develops in the connection zone between the CFS frame and the sheathing board whilst failure of chord studs and Hold-Down elements is prevented through capacity design. Given the fact that EC8 does not provide guidance on the design of CFS-SWP lateral load resisting system, in this study the design of this structural system is carried out following a design procedure tailored to the framework of EC8 [25], adopting a behaviour or response modification factor (q) equal to 2. As for the design of non-dissipative elements (track, stud, chord stud and Hold-Down), capacity design rules for thin-walled members provided in Part 1.3 of Eurocode 3 (EC3) [26] are adopted herein. Since the CFS profiles are made of slender cross-sections (Class 4 according to EC3 classification), local buckling is expected to occur before the attainment of the yield stress in one or more parts of the cross-section. Either the Effective Width Method (EWM) or the more accurate Direct Strength Method (DSM) [27] could be used to evaluate their axial and flexural design strengths in order to take into account the strength reduction resulting from the development of buckling effects (local, distortional and global). Further details on the seismic design procedure for CFS-SWP system and its performance factors can be found in the work of Kechidi et al. [25].

2.2. Steel moment-resisting frames

The response of a conventional steel MRF depends on the characteristics of its fundamental components namely the columns, beams and connections (*e.g.,* beam-to-column connection). In this structural system, the shear yielding of the panel zone as well as the flexural yielding of the beams represent the main source of energy dissipation. In this study, the MRFs have been firstly designed to resist gravity loads in accordance with the provisions of EC3 [28] for sectional resistance, stability checks and deflection serviceability limits. Afterwards, seismic design was performed in accordance with the EC8 provisions considering a behaviour factor (q) equal to 4. Two limit states were verified, namely damage limitation and ultimate limit states. Although it is not specifically defined in EC8 [1], it is considered by the authors that the first step of the design process should be the DL limit state checking, particularly in the case of flexible structures located in moderate-to-high seismicity regions (see Section 3). Regarding the NC limit state, the design process consists of checking the dissipative elements followed by capacity design of non-dissipative elements. The capacity design of the non-dissipative members was conducted according to the EC8 criteria with the modifications proposed by Elghazouli [29]. As for the design of the panel zone, a "balanced" design approach was adopted in this study [30] which establishes that panel zones should be proportioned such that yielding of these elements occurs at similar load levels that develop flexural plastic hinges in the beams. The potential influence of second-order P-Δ effects should be checked through the calculation of the inter-storey sensitivity coefficient θ. In this study, the θ coefficient was limited to 0.2, meaning that an amplification of the lateral load had to be performed during the design process [1]. Furthermore, the DL performance requirement was considered in the seismic design by limiting the inter-storey drift ratio during a frequent earthquake event to 1% of the storey height.

3. Selection and design of the buildings

Two-, 4- and 5-storey CFS-SWP and MRF buildings have been selected and then designed. Table 1 summarizes the parameters used to describe the design space where two sites located in Portugal, namely Porto (north) and Lagos (south) were considered to reflect, respectively, low and moderate-to-high seismicity regions. The acceleration and displacement elastic response spectra are plotted in Fig. 1. The storey heights of CFS-SWP and MRF systems are 2.74 m and 3.50 m, respectively, with a MRF first floor height equal to 4.50 m.

A simple floor plan was selected for the buildings studied herein (Fig. 2). For the CFS-SWP system, rectangular buildings with perimeter shear walls that resist lateral forces for each direction intending to represent a typical CFS structure where the length of the lateral load resisting system is proportional to the lateral demand (Fig. 2a). As for the MRF system, the structural configuration in plan is shown in Fig. 2b. The buildings consist of three MRFs spaced at 6 m. Resistance to seismic loads is provided by the three frames in the longitudinal

Table 1
Parameters of the design space for CFS-SWP and MRF systems.

Building	Number of storeys	Design load level	
		Occupancy	Seismicity
1	2	Residential	Low (PGA = 0.8 m/s^2, soil class B)
2	4		
3	5		
4	2		Moderate-to-high (PGA = 2.5 m/s^2, soil class C)
5	4		
6	5		

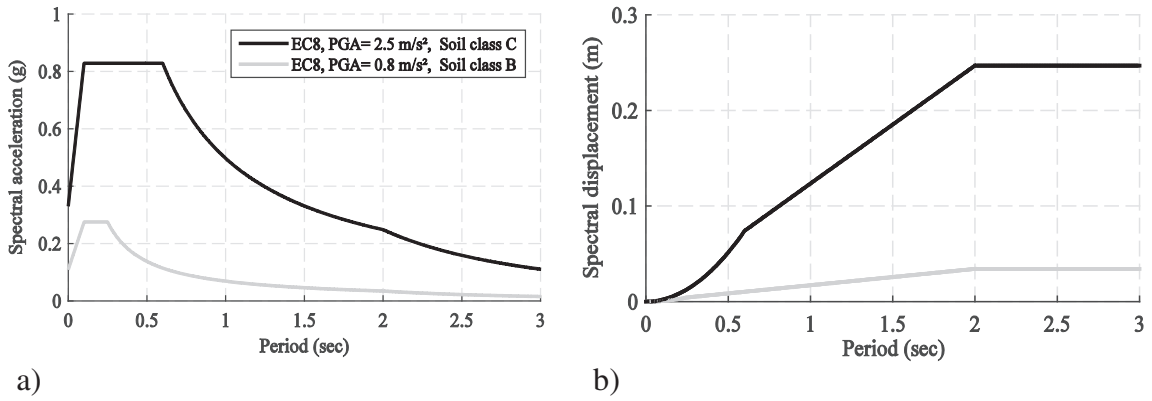

Fig. 1. EC8 elastic response spectra for the two seismic intensity levels: a) acceleration and b) displacement.

direction and by a bracing system in the transverse direction. As depicted in Fig. 2, the building structures are analysed in the longitudinal (horizontal) direction.

Live loads of 2.0 kN/m^2 and 1.0 kN/m^2 were applied on the intermediate and roof floors, respectively. The seismic mass was derived through conversion of the vertical loads corresponding to the quasi-permanent combination.

A solution to minimize the length of SWPs is to employ double-sided sheathing. However, the axial force demand on chord studs increases. Hence, there was a need for thicker framing members (2.583 mm) in comparison to the common range (0.879 to 1.438 mm). The challenging issue was to delay the chord studs' failure. The physical and mechanical properties of the built-up chord stud made by two lipped C-sections 362S162 per AISI S200 nomenclature [31] (nominal dimensions: 92.08 mm (web) × 41.28 mm (flange) × 12.7 mm (lip)) connected back-to-back (Table 2) have been adopted to design chord stud members. Material properties of the CFS members are as follows: for members with thickness lower than 1.146 mm, the minimum yield strength of steel was 228 N/mm^2. Members having thickness greater or equal to 1.438 mm were considered to be made from steel with minimum yield strength of 340 N/mm^2.

Table 4 summarizes the resulting CFS-SWP configurations and the chord stud sections for each CFS structure. The design process primarily consisted in selecting the SWP in terms of the required configuration (Table 3) that satisfies the design provisions outlined in Section 2.1, as well as the capacity design of the chord stud and Hold-Down elements. Moreover, the structural period-based ductility (μ_T) and lateral overstrength (Ω_0) were evaluated according to the FEMA P695 criteria [32] for all buildings of both structural systems from nonlinear static analyses (see Section 5.1).

As for MRFs, European HEB and IPE cross-sections were adopted for the columns and beams sections, respectively, assuming a yield strength of 275 N/mm^2. The calculated cross-sections sizes, obtained based on the design procedure detailed in Section 2.2, are listed in Table 5.

The design procedure for the MRFs at both seismic intensity levels led to similar structural element sizes (beams and columns cross-sections). The main reason behind these design outcomes is the fact that the second order stability effect (P-Δ) was the governing design criterion rather than strength requirements as opposed to CFS-SWP structures, where their design was mostly governed by strength demands. Particularly, in the case of buildings designed for a low seismicity site (Porto), the calculated shear demand was much smaller than the minimum possible SWP shear capacity, which resulted in a relatively higher lateral overstrength (stiffness) of the whole system in comparison to those of the same system (CFS-SWP) designed for the sites corresponding to moderate-to-high seismicity (Table 4). Since the governing design criterion of the MRFs is primarily a drift restriction (P-Δ) due to their relatively high ductility, the resulted static overstrength factors (Table 5) are much higher than those of CFS-SWP structures. The obtained solutions for both structural systems are now

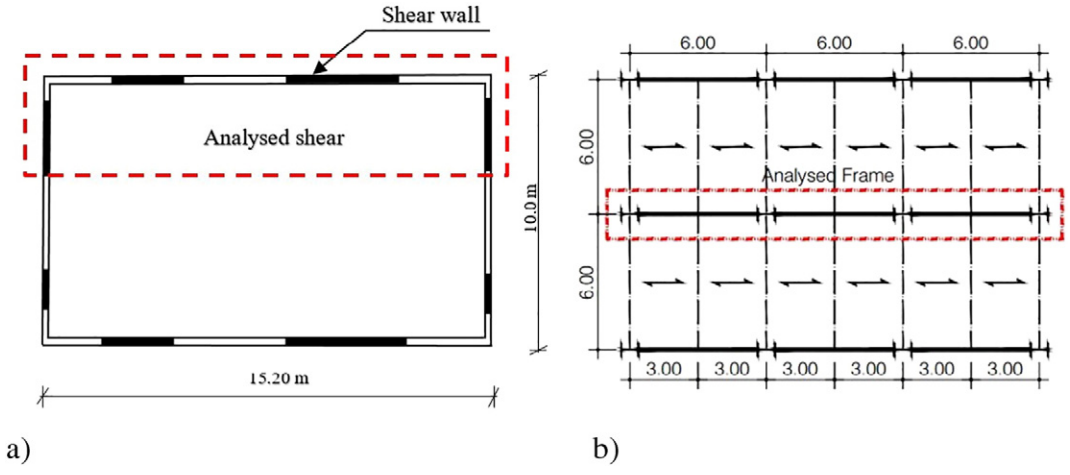

Fig. 2. Plan view of: a) CFS-SWP and b) MRF buildings.

Table 2
Chord stud cross-sections properties.

Chord stud sections	Thickness (mm)	fy (MPa)	A (mm^2)	I_x (mm^4)	I_y (mm^4)
1	1.146	228	438.4	590,868	295,434
2	1.438	340	544.4	726,506	363,253
3	1.811	340	675.7	889,635	444,817
4	2.583	340	934.2	1,194,415	597,207

compared in terms of their weight. Fig. 3 shows the weight of each solution.

It is clear from Fig. 3 the difference in steel weight between CFS-SWP and MRF systems. From these results, it is possible to conclude that CFS-SWP system uses approximately 15% of the steel weight found in its MRF counterpart. It is worth noting that the above-mentioned weight ratio was determined on the basis of merely the lateral load resisting system components rather than all building components such as the floor diaphragms, vertical load bearing walls, partition walls, exterior and interior finishes, fire protection *etc.* Moreover, it should be noted that this significant difference in weight resulted in structures with very different dynamic characteristics, as demonstrated by the fundamental periods of vibration listed in Tables 4 and 5. In general, CFS-SWP structures have lower periods of vibration than MRFs (particularly those designed for Lagos) and hence are expected to develop lower levels of deformations.

4. Numerical modelling and seismic action

The key aspect in conducting a probabilistic seismic performance assessment is the accurate estimation of the nonlinear structural response with the least rate of uncertainty which is a twofold issue: (i) the formulation of reliable numerical models, and (ii) the adoption of ground motion records that are consistent with the seismic hazard of the site for which the seismic design was carried out.

4.1. Modelling approaches

The OpenSees finite element (FE) software [21] has been adopted in this study to model the structural systems and to conduct nonlinear static and dynamic analyses.

4.1.1. Sheathed CFS-SWP system

The central challenge in performing the assessment of the structural performance under seismic loading is the development of robust, yet computationally efficient, models that can be used to accurately simulate the nonlinear dynamic response history of the structure when subjected to increasing seismic demands. Recent research carried out by Kechidi and Bourahla [33] has resulted in a novel material model that has been implemented in OpenSees and which is designated by "CFSWSWP" uniaxialMaterial. The model is capable of simulating the deteriorating behaviour, strength degradation (both cyclic and in-cycle), stiffness degradation as well as the pinching effect of sheathed CFS-SWP associated with sheathing-to-framing fasteners damage that are critical in sidesway failure mode. This hysteresis model has been validated against experimental test data [2] and is available in the OpenSees software version 2.4.5 and above [34]. Schematic drawings of the numerical models are provided in Fig. 4b.

The overall lateral stiffness and strength of the CFS-SWP are modelled using a concentrated plasticity hinge (CPH) approach. An equivalent zeroLength element is located at the centre of the SWP with CFSWSWP uniaxialMaterial and connected to rigid truss elements that transmit the force to the chord studs that are modelled with elasticBeamColumn elements. The framing members have pinned ends so that they do not develop any resistance to lateral loads. The structural members not contributing to the lateral stiffness (bearing and partition walls) are considered by connecting one leaning column to the CFS-SWP frame. In order to ensure a proper distribution of seismic forces among all SWPs, a multipoint constraint is used to slave the horizontal degree of freedom at each floor level to simulate a rigid diaphragm. P-Δ geometric transformation is applied for proper consideration of geometrical nonlinear effects [25].

4.1.2. Steel moment-resisting frames

As for MRFs, beams and columns are represented with an elasticBeamColumn element. The material nonlinear behaviour is considered through a CPH approach in which column and beam ends are assigned a hysteretic behaviour that takes into account strength and stiffness deterioration effect (Lignos and Krawinkler [35]). Fig. 5 illustrates an example of a backbone curve and hysteresis loops for an European HEB 300 profile along with the stiffness and deterioration parameters that have been calibrated following the procedure proposed by Araújo et al. [36]. The effect of the axial load on the flexural capacity of the columns was taken in an approximate way. A preliminary pushover analysis has been conducted first in order to evaluate the expected average axial force under the combined actions of gravity and lateral loading as follows: $P_{grav} + 0.5 \times P_E^{max}$, where P_{grav} and P_E^{max} are the axial force due to gravity loads and the maximum axial force due to lateral loading, respectively (Zareian et al. [37]). Consequently, the backbone curve is adapted by reducing the flexural strength according to interaction equations proposed in EC3-1-1 [28]. However, no modification of the stiffness and deterioration parameters is made in this approach. On the other hand, the panel zones are modelled using a beam-column joint element "Joint2D" that is available in OpenSees. The rotational spring utilized to represent the panel zone is assigned

Table 3
Design parameters of SWP elements.

Test label	Wall Size H/W[a] (mm/mm)	Fastener spacing[b] (mm)	Track thickness (mm)	Ultimate shear strength (kN)	ASD[c] design strength (kN)	LRFD[d] design shear strength (kN)
1	2440/3660	152/305	1.12	60.763	30.382	42.534
2	2440/3660	102/305	1.12	87.002	43.501	60.901
3	2440/3660	76/305	1.12	115.555	57.778	80.889
4	2440/3660	50/305	1.12	169.445	84.723	118.612
5	2440/2440	152/305	1.12	35.915	17.958	25.141
6	2440/2440	102/305	1.12	54.431	27.216	38.102
7	2440/2440	76/305	1.12	72.061	36.031	50.443
8	2440/2440	50/305	1.12	105.761	52.881	74.033

[a] Height-to-width aspect ratio.
[b] Screw fasteners spacing at perimeter/centre of the SWP.
[c] Design strength for Allowable Stress Design (ASD);
[d] Design strength for Load and Resistance Factor Design (LRFD).

Table 4
CFS-SWP structural system design parameters.

Building ID	T_1 (sec)	SWP type (defined in Table 3)		Chord stud thickness (mm) (defined in Table 2)	Design criterion	Ω^c	μ^c
		1st bay (2440 mm)	2nd bay (3660 mm)				
1	0.35	6[a]/5	NA[b]	1[a]/1	Resistance	2.1	5.03
2	0.93	6/6/5/5	NA	2/1/1/1	Resistance	2.77	3.77
3	1.14	7/6/5/5/5	NA	2/2/1/1/1	Resistance	3.05	3.42
4	0.25	7/5	3/1	2/1	Resistance	1.77	5.44
5	0.37	77[d]/77/8/5	33/33/4/1	4/3/2/1	Resistance	1.54	3.65
6	0.42	88/88/77/8/5	44/44/33/4/1	4/4/3/2/1	Resistance	1.54	3.35

[a] From the bottom to the top of the building.
[b] Not applicable: lateral load resisting system composed of only one SWP line.
[c] Static pushover analysis outcomes.
[d] Double number means double-sided sheathing in SWPs.

the Krawinkler [38] tri-linear moment-distortion behaviour. It is worth noting that no deterioration has been considered for the panel zone behaviour. Fig. 6 illustrates the adopted modelling strategy for the performance assessment of MRFs. Gravity loads were applied to the model as initial loads.

4.2. Seismicity and ground motion record selection

The SelEQ tool (Macedo and Castro [40]) was employed to derive the CMS for each of the selected sites and structures, for a probability of occurrence of 5% in 50 years (return period of 975 years). Since the spectral shape changes with the intensity level, a selection of multiple sets of records at multiple intensity measure levels is required to account for such changes in the spectral shape and use multiple stripe analysis "MSA" instead of IDA. In this study, a simplified approach was assumed adopting a single intensity level of 5% in 50 years corresponding to an intermediate level between 2% and 10% in 50 years (return period of 2475 and 475 years, respectively). It is worth noting that, for the Portuguese territory, the seismic hazard model developed in the SHARE research project [41] was used in combination with additional hazard (Vilanova and Fonseca [42]). The ground motion prediction equations considered were Atkinson and Boore [43] and Akkar and Bommer [44] with a weight of 70% and 30%, respectively (Silva [45]). The exact CMS incorporating aleatory and epistemic uncertainties has been computed and used as a more realistic target response spectrum for the ground motion record selection. Further details regarding the calculation of the CMS can be found in the work of Lin et al. [46]. Sets of 40 ground motion records obtained from real earthquake events were selected for each structure from the PEER strong motion database [47] and scaled to match the mean and standard deviation of the previously calculated CMS (Fig. 7).

The response spectrum prescribed in current building codes is often a Uniform Hazard Spectrum (UHS). Fig. 8 shows the UHS for Porto (left) and Lagos (right) along with the elastic response spectra of EC8 as well as the Conditional Mean Spectrum obtained in this study. The UHS have been validated against the results of the SHARE project which are available at EFEHR [41].

One can notice discrepancies between the elastic response spectra defined in EC8 for Porto and Lagos and the UHS (5%/50 years). This is because the Hazard Models and GMPEs used in the UHS computation are different from the background data adopted in the development of the elastic response spectra of EC8 for the Portuguese territory. It is worth noting that the data employed in the UHS computation is based on the most recent and available hazard models developed for Europe [41].

5. Nonlinear analyses

5.1. Lateral behaviour

Nonlinear static analysis (pushover) was carried out under displacement control on all structures of both systems in order to evaluate their lateral behaviour. To initiate the analysis, the lateral loads were distributed along the height of the structures following a lateral load pattern proportional to the first-mode of vibration of the structures. Before running the analysis, the models have been subjected to initial loads corresponding to the gravity loads. Fig. 9 shows an example of pushover curves of CFS-SWP and MRF 5-storey structures designed for the Lagos site.

Table 5
MRFs design parameters.

Building	T_1 (sec)	Floors	Beams	Interior columns	Exterior columns	Design criterion	Ω^b	μ^b
1/4[a]	0.81	1	IPE300	HEB 240	HEB 200	P-Δ/resistance	21.97/3.04[c]	6.56
		2	IPE300	HEB 240	HEB 200			
2/5	1.07	1	IPE330	HEB 360	HEB 300	P-Δ	22.26/3.13	5.56
		2	IPE330	HEB 360	HEB 300			
		3	IPE300	HEB 320	HEB 280			
		4	IPE300	HEB 320	HEB 280			
3/6	1.18	1	IPE400	HEB 360	HEB 320	P-Δ	20.16/3.12	6.52
		2	IPE360	HEB 360	HEB 320			
		3	IPE330	HEB 340	HEB 320			
		4	IPE300	HEB 340	HEB 320			
		5	IPE300	HEB 320	HEB 300			

[a] Similar design (columns and beams cross-sections) for both buildings.
[b] Static pushover analysis outcomes.
[c] Two separated numbers correspond to the results of buildings having same number of storeys design for low/moderate-to-high seismicity regions.

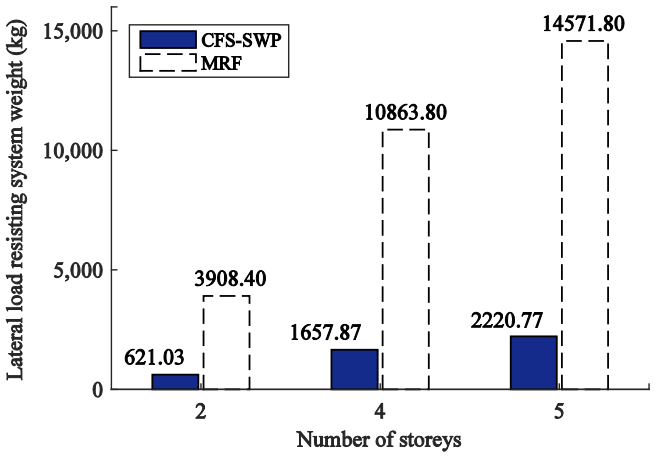

Fig. 3. Lateral load resisting system weight of CFS-SWP and MRF systems designed for Lagos site.

As opposed to the MRF system, for which the behaviour is linear elastic at low loading level, Fig. 9a shows that the CFS-SWP system exhibits nonlinear behaviour at very low lateral displacements. This characteristic is due to the behavioural complexity of the SWP components and their interaction (see Fig. 4a).

The difference in ductility between the two systems is obvious in Fig. 9. This can be attributed, in part, to the design and modelling assumption made for CFS-SWP system, where the chord studs are not continuous along the height of the structure [25]. Additionally, the fact that SWPs are the only lateral load resisting elements of CFS-SWP building system, a clear post-peak drop of the structure's lateral capacity is observed. This contributes to a low level of redundancy of the structural system, which significantly results in a concentration of inelastic demands, notably after failure of one SWP, which ultimately triggers the development of global collapse. Conversely, the capacity curve of the MRF system (Fig. 9b) after global yielding is much more stable where plasticity develops gradually in its elements (beams and columns) which lead to a high level of global ductility. The source and level of lateral overstrength observed for both structural systems has been discussed in Section 3.

5.2. Dynamic response

The characterization of the seismic performance of the structures is carried out based on a large number of nonlinear dynamic response history analyses (*e.g.*, 1000 runs for building 1 of the CFS-SWP system) under the sets of ground motion records previously selected, scaled to several intensity levels, known as IDA [48]. Accordingly, various response characteristics under low- and high-shaking intensities are represented.

In this study, and in order to generate the response parameters required for the derivation of the fragility curves, the building models have been subjected to ground motion records sets (40 records per set following the selection procedure described in Section 4.2) scaled for increasing intensity levels until collapse of the structures. Additional analyses are typically performed within the last interval of intensities to determine, as accurately as possible, the collapse intensity within a certain tolerance. In this paper, the 5% damped first mode pseudo-spectral acceleration Sa (T_1, 5%) (as an abbreviation, Sa (T_1) will be used hereafter) is used as the intensity measure. The term collapse adopted in this study, for both lateral load resisting systems, corresponds to the attainment of 10% of the initial slope of the mean of the IDA curves. Since in CFS buildings the SWP is the primary element for resisting the lateral loads, the engineering demand parameter (EDP) was defined as the lateral drift of the SWP which coincides with the inter-storey drift. Values of inter-storey drift equal to 1.0% and 2.1%

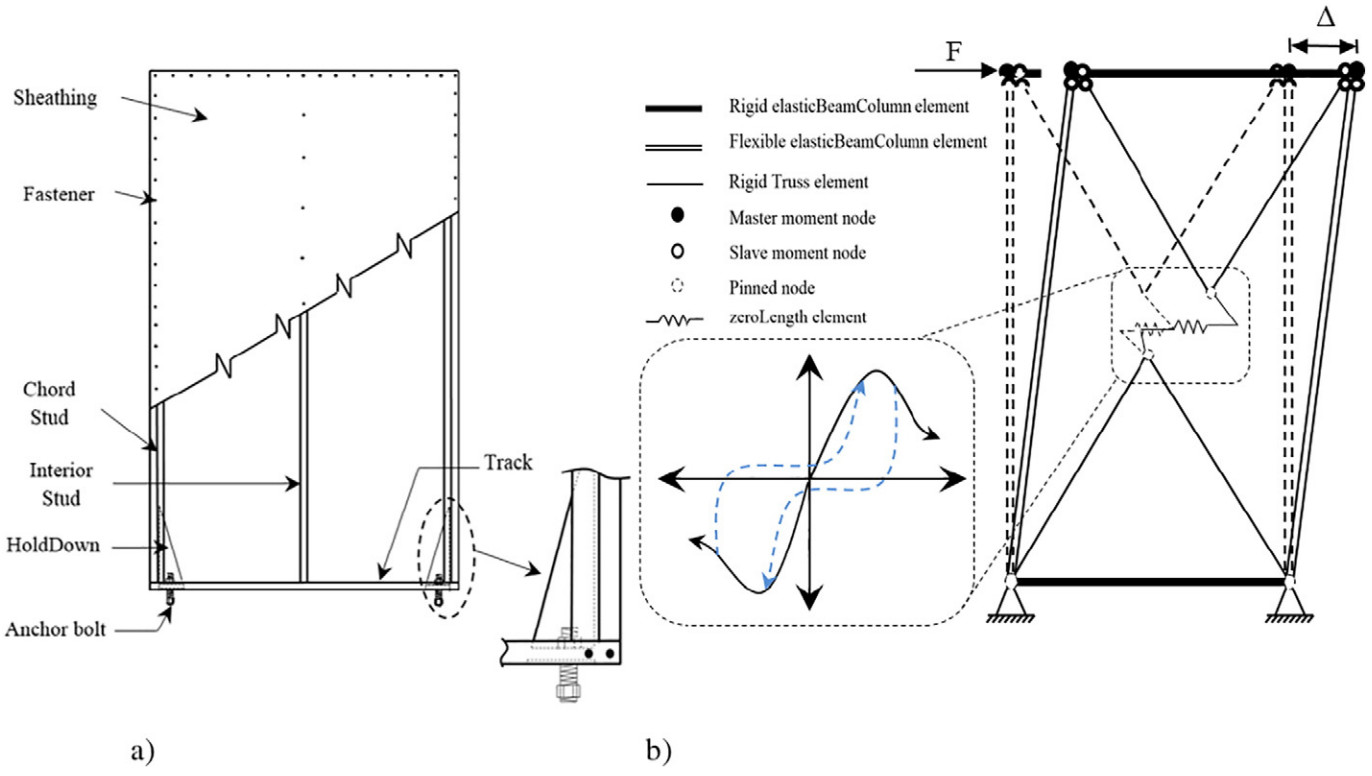

Fig. 4. CFS-SWP system: a) main components and b) OpenSees FE model using concentrated plasticity approach [34].

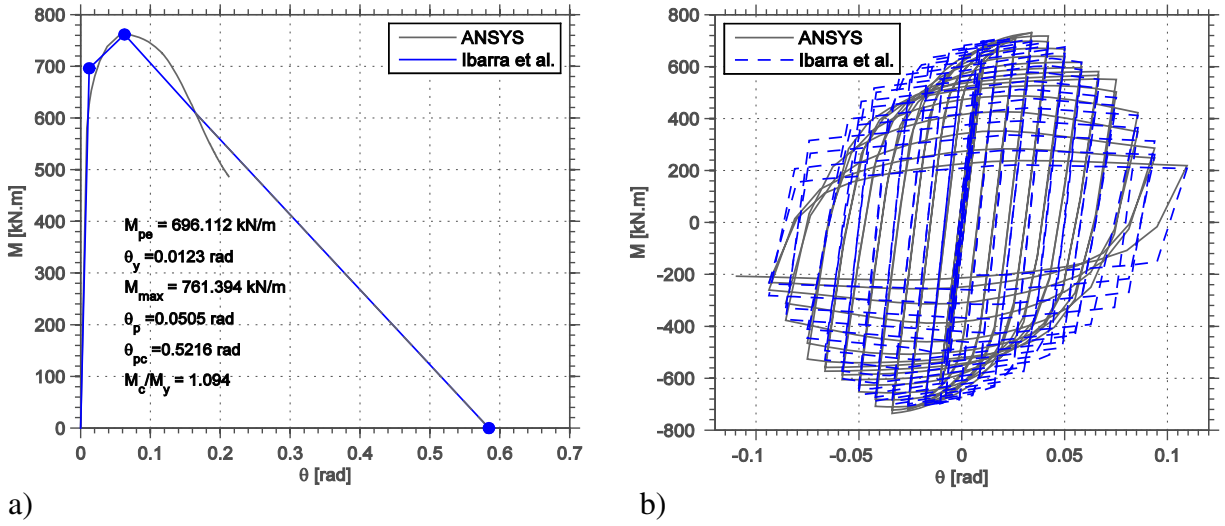

Fig. 5. Calibration of the Modified Ibarra–Krawinkler deteriorating model for an HEB 300 steel profile: a) monotonic and b) cyclic behaviour.

were adopted for the definition of the DL and NLC limit states (performance levels), respectively. These values were based on the study performed by Martinez (2007) [49]. Moreover, the lateral drift of a SWP might be lower than the limit value for a given performance level but the internal forces installed on the chord studs might exceed their capacity. Therefore, to determine whether or not the lateral capacity of the SWP has been exceeded, both the SWP lateral drift and strength demand on chord studs have been monitored in all response history analyses. As for MRFs, to be consistent in the comparison and to avoid bias in the results, the inter-storey drift ratio has also been adopted as the EDP. Inter-storey drift ratio limits of 1.0% and 2.5% were considered as per ASCE 41-13 [50] corresponding to the above described two limit states.

The PoE was calculated, based on the IDA results, as the ratio of ground motion records that caused the exceedance of a given performance level at each intensity measure level to the total number of ground motion records (40 records). A lognormal cumulative distribution function (CDF) was used to define a fragility curve. The evaluation of the fragility function parameters was based on the Maximum Likelihood Estimation method proposed by Baker [51]. Figs. 10 and 11 show the fragility curves obtained for the DL limit state for both CFS-SWP and MRF structures, respectively, in which the x-axis is normalised to Sa (T_1) of the EC8 elastic response spectrum for the serviceability limit state level.

The results presented in Figs. 10 and 11 show that the probability of both structural systems exceeding the limit imposed at the design stage (EC8, 1% inter-storey drift) is extremely low. They also indicate that, for low- to medium-rise buildings, located in low and moderate-to-high seismicity regions, the CFS-SWP system provides an acceptable serviceability (functionality) performance.

Fig. 11 shows a reduced standard deviation in the fragility curves of MRFs corresponding to DL limit state. This is explained with the low levels of plasticity that develop in the structures for the seismic intensity level considered, with the regularity of the structural system which has more than 90% of the effective modal mass being mobilized at the first-mode period of vibration (this holds true for CFS-SWP system as well),

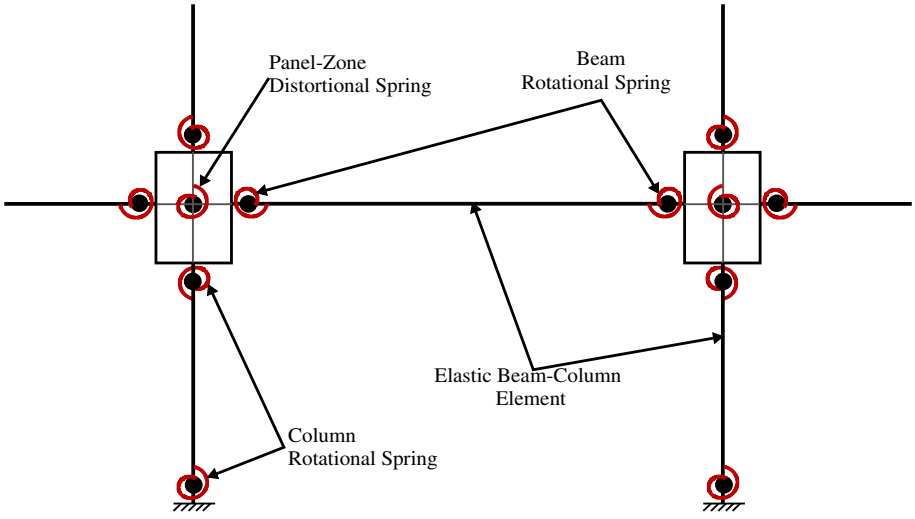

Fig. 6. OpenSees FE model of steel MRF: joint zone, column and beam ends represented by rotational springs [39].

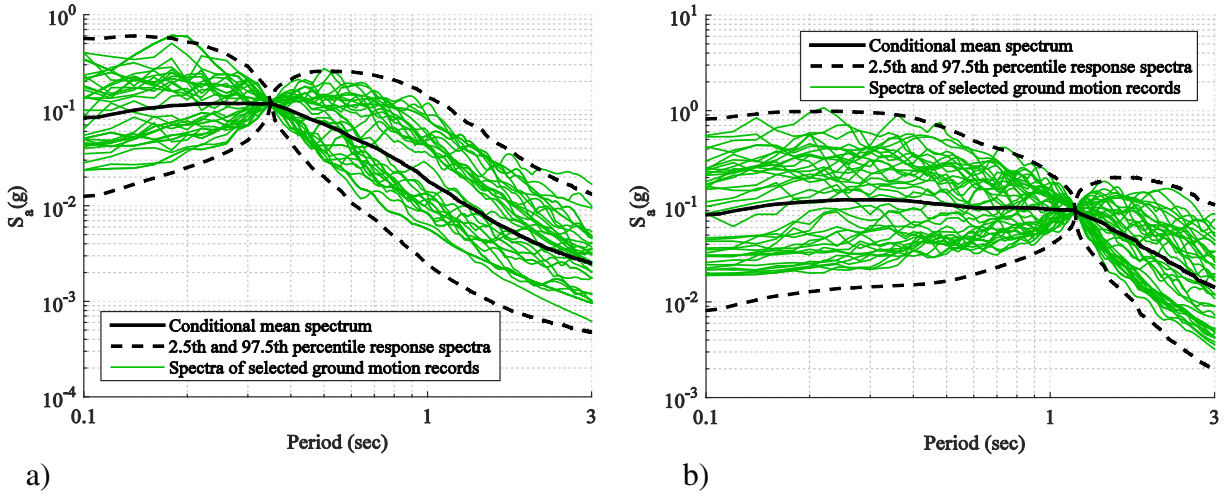

Fig. 7. Response spectra of selected ground motion records for: a) Sa ($T_1 = 0.35$ s, Porto) and b) Sa ($T_1 = 1.18$ s, Lagos) having 5%/50 years probability of occurrence.

and, importantly, with the reduced spectral variability of the selected ground motion records at the fundamental period of vibration. On the other hand, for the CFS-SWP system, the fragility curves for the DL limit state are characterized by relatively higher standard deviations (Fig. 10). This is justified with the inelastic behaviour of the structural system for low levels of lateral deformation, as discussed in Section 5.1, in addition to the deteriorating characteristics of the hysteretic behaviour of the CFS-SWP system, which results in the lengthening of the first-mode period of vibration from early stages of the earthquake response. Therefore, the PoE are more sensitive to the spectral shape effect in the case of CFS-SWP system than in the MRF structural system. This emphasizes the fact that the impact of adopting the CMS, as a target spectrum for ground motion record selection, on the structural response varies depending on the characteristics of the structures being analysed in this study. Nevertheless, the generalisation of this conclusion can only be made based on a detailed study conducted over different building types and intensity measures. As for the NLC and NC limit states, the corresponding results are shown in Figs. 12 and 13 for CFS-SWP and MRF structures, respectively, in which the x-axis is normalised to Sa (T_1) of the EC8 elastic response spectrum.

Similarly, when the performance of both systems is compared for the NLC and NC limit states, low levels of PoE are observed. Slightly higher values are obtained for the CFS-SWP system in comparison to the MRF system. The reason behind this observation is found on the different values of inter-storey drift that were adopted to characterize the NC limit state for both structural systems (5% inter-storey drift for the MRF as opposed to 2.5% for the CFS-SWP system). It is worth noting that there is also a clear difference in terms of the global ductility of both structural systems (see Section 5.1). Moreover, the fragility curves of CFS-SWP system for NLC and NC limit states are similar in terms of median and standard deviation, which indicates that the EDP adopted in this study represents, jointly, the local and global collapse for this structural system, which reveals once more the low level of redundancy of the CFS-SWP system as discussed in Section 5.1.

The results depicted in Figs. 12 and 13 illustrate the consequence of a drift-controlled seismic design. It is clear that the MRFs exhibit a reserve of strength which is reflected in a resistance against collapse for seismic intensities corresponding to more than two times the design earthquake intensity level (Fig. 12). A similar good performance is also observed for the CFS-SWP system (Fig. 13). Additionally, these results demonstrate the reliability and effectiveness of the proposed seismic design procedure and the suitability of adopting a behaviour factor q equal to 2 for the CFS-SWP system as suggested in the work of Kechidi et al. [25], where performance groups designed for Lagos site have not fulfilled the FEMA P695 acceptance criteria under Maximum Considered Earthquake level. Following the CMS approach in selecting ground motion records set showed a superior structural performance when compared to FEMA P695-based results [25]. This proves the influence

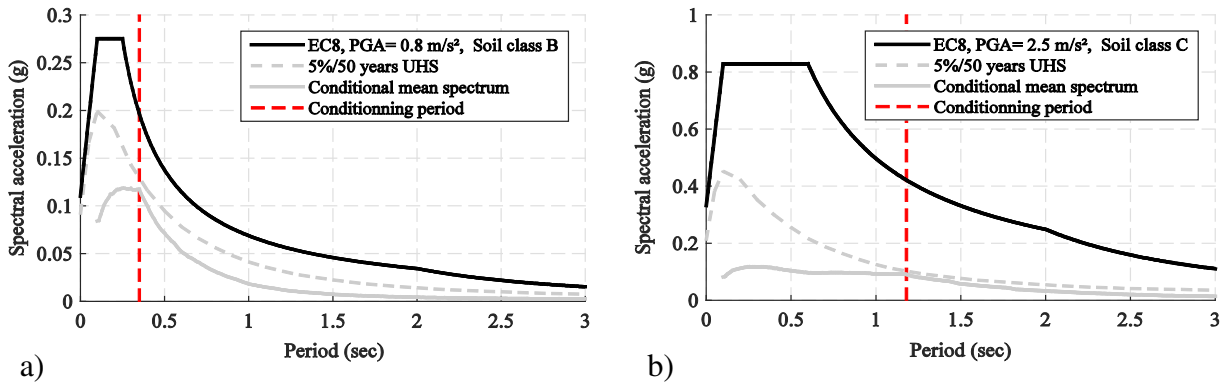

Fig. 8. EC8 elastic response spectrum, 5%/50 years UHS and CMS for: a) Porto and b) Lagos.

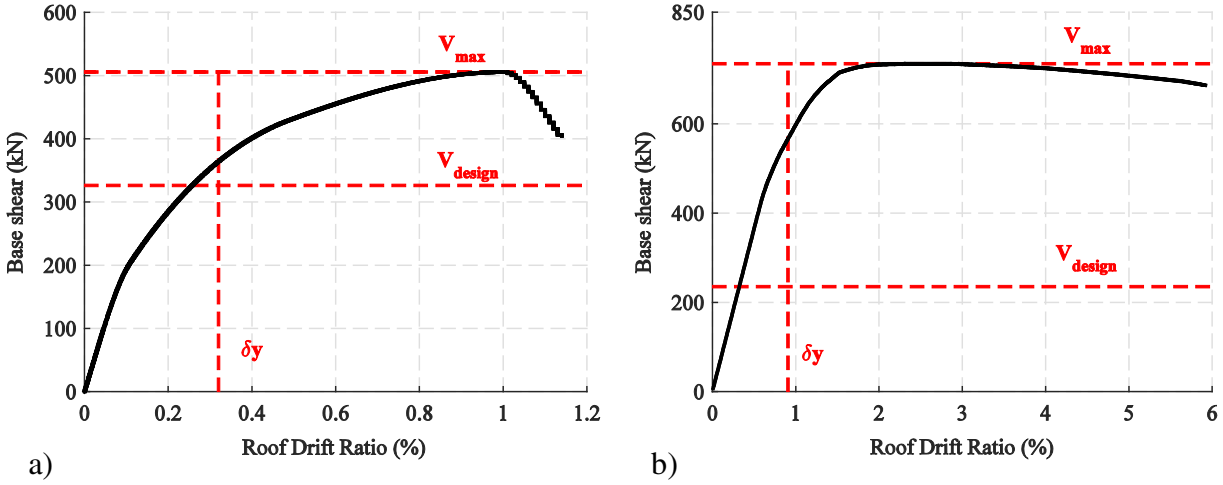

Fig. 9. Pushover capacity curves of building 6: a) CFS-SWP and b) MRF systems.

of the spectral shape effect on the seismic performance of the buildings and draws attention to the consequences of deviating from the target CMS when selecting sets of ground motion records. A similar conclusion has been drawn by Haselton and Baker [52]. All the observations made above regarding the fragility curves are expected to have an important impact on the quantification of the seismic risk, which is presented in the following section.

6. Seismic risk assessment

Despite the differences in the fragility curves that have been identified in the previous section, the effectiveness of each structural system for seismic resistance can only be fully assessed based on the evaluation of the seismic risk. The fragility curves of the studied structures are combined with site-specific hazard curves representing the

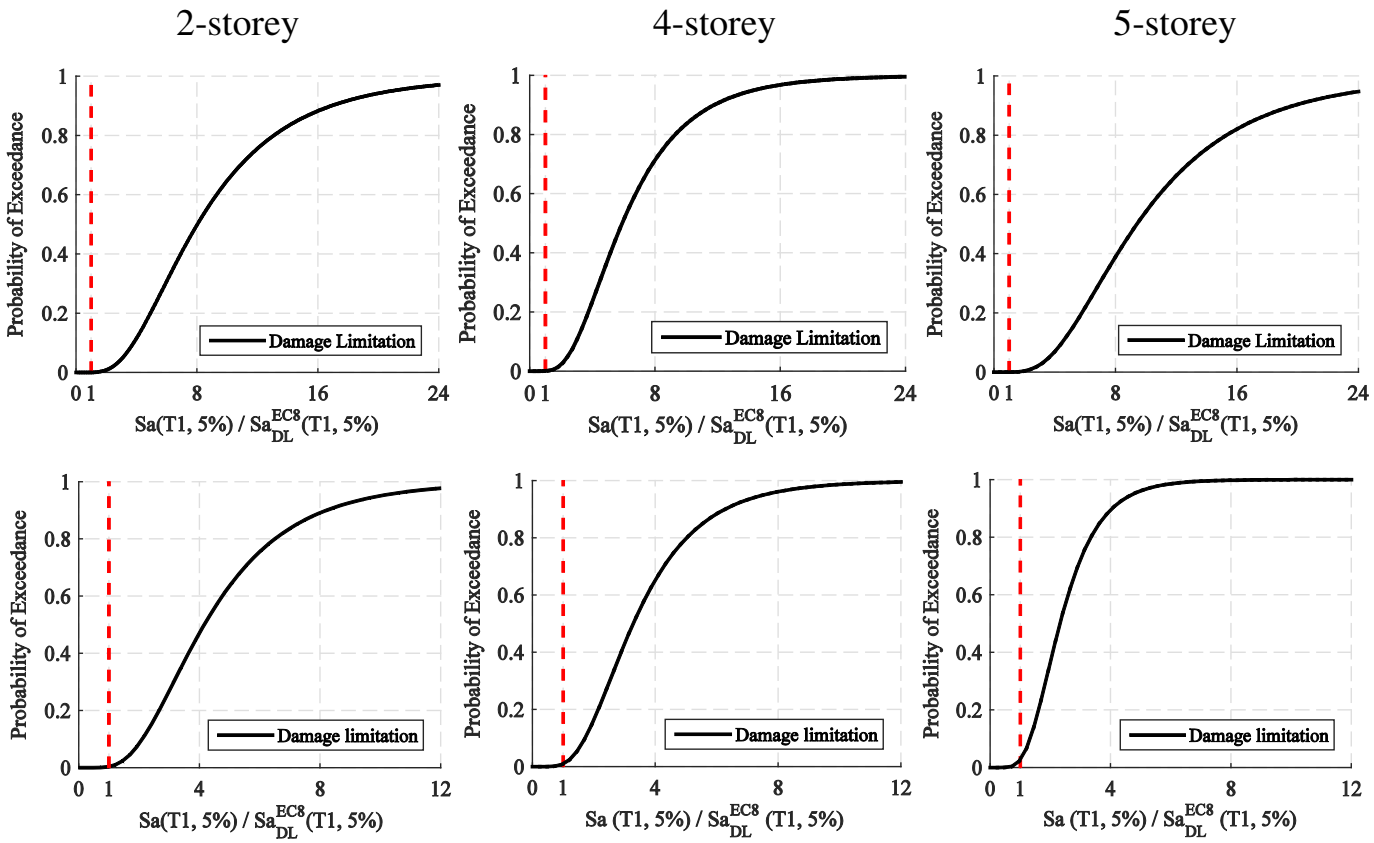

Fig. 10. DL limit state fragility curves of the CFS-SWP structures designed for: Porto (top) and Lagos (bottom).

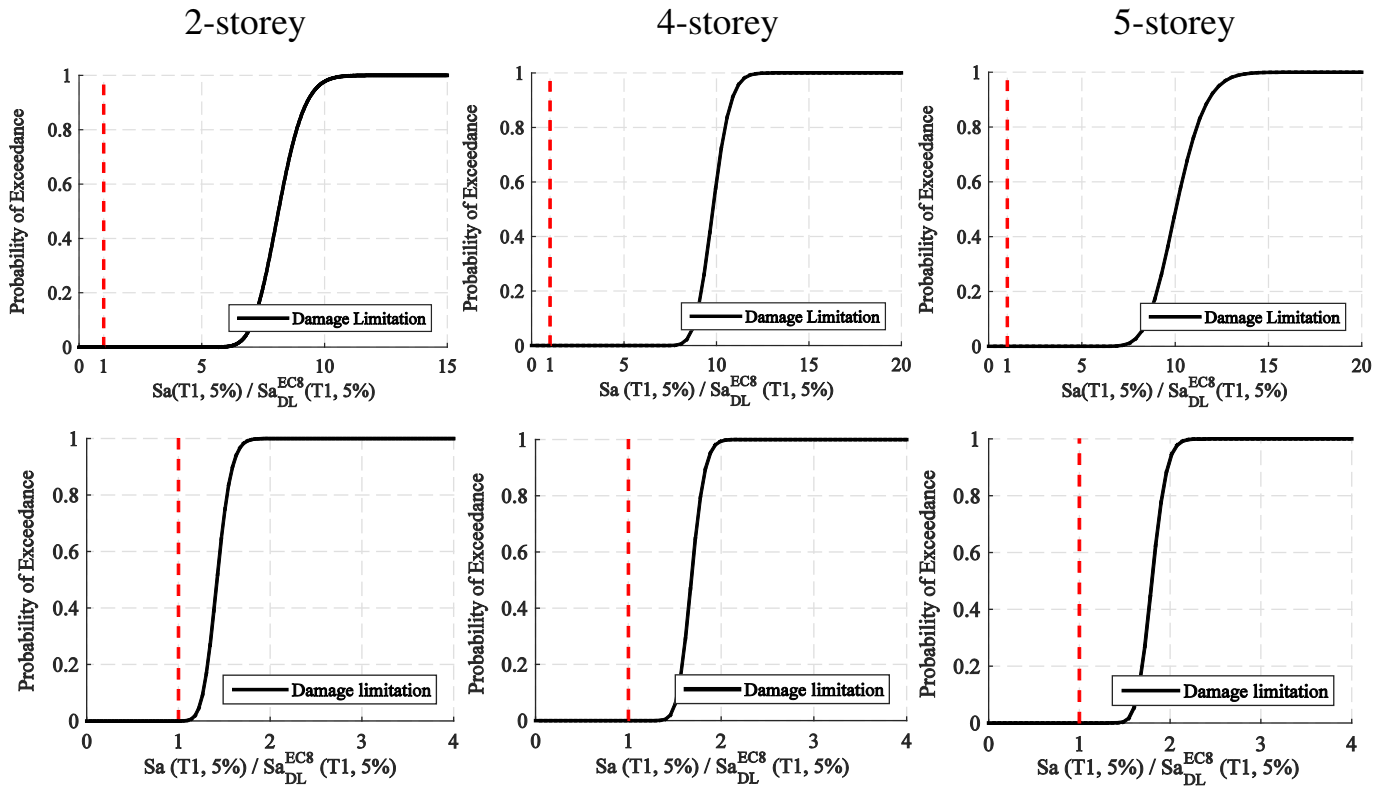

Fig. 11. DL limit state fragility curves of the MRF structures designed for: Porto (top) and Lagos (bottom).

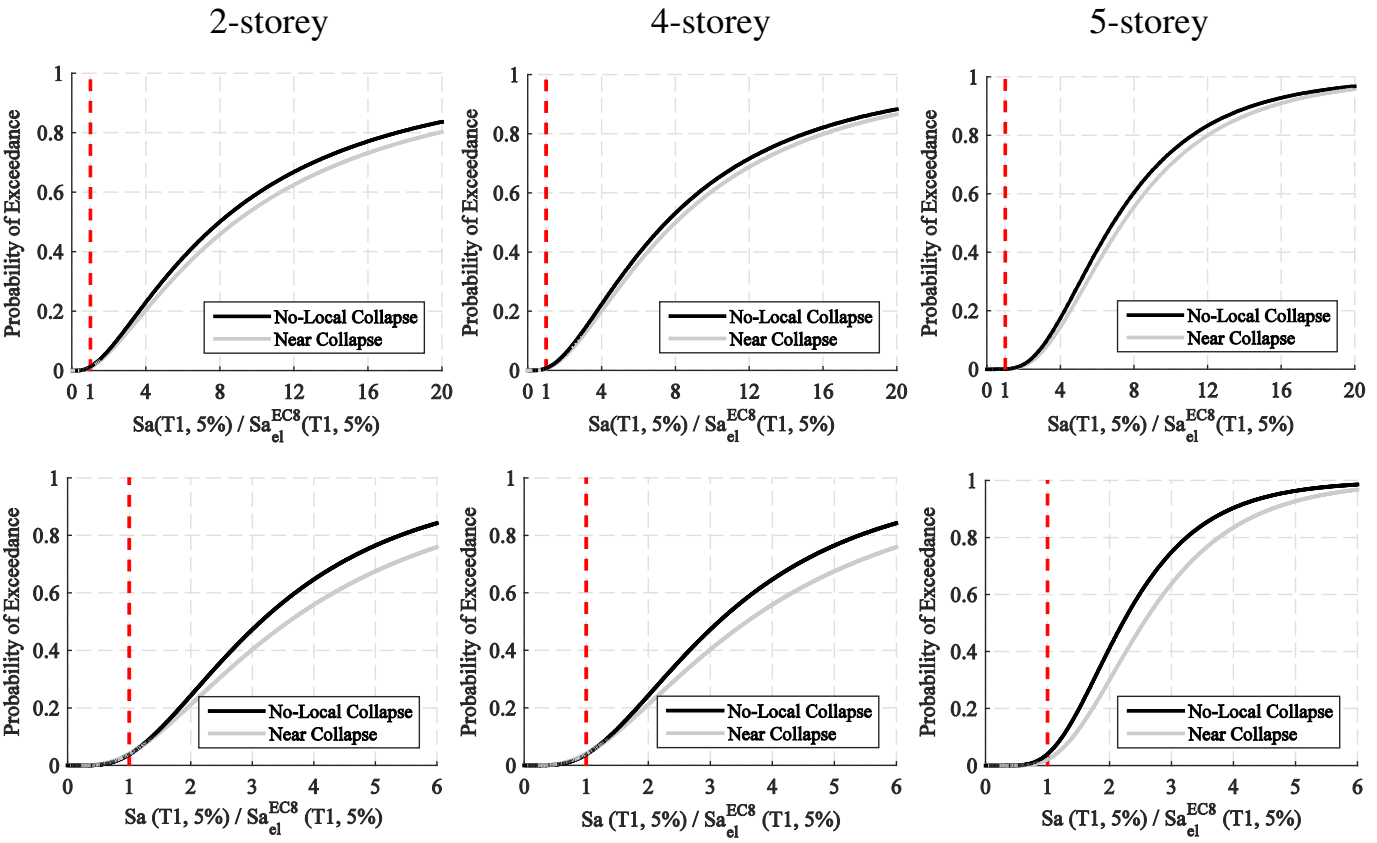

Fig. 12. NLC and NC limit states fragility curves of the CFS-SWP structures designed for: Porto (top) and Lagos (bottom).

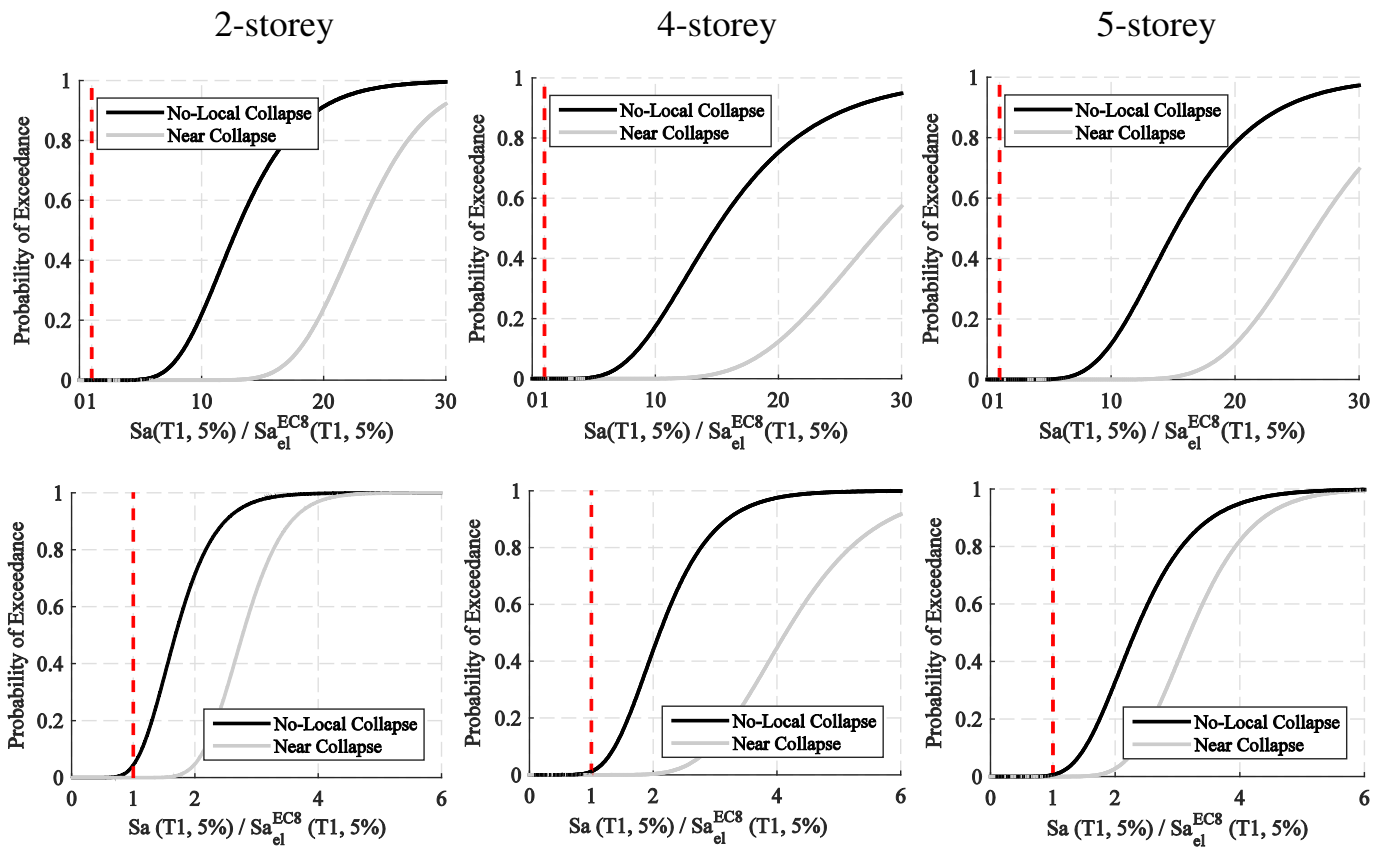

Fig. 13. NLC and NC limit states fragility curves of the MRF structures designed for: Porto (top) and Lagos (bottom).

probability of occurrence of earthquake intensities within a specific timeframe (Fig. 14). The seismic risk is quantified in terms of the mean annual probability of exceeding the above described limit states (λ_{DL}, λ_{NLC} and λ_{NC}). Computing λ_i involves the integration of the fragility curve over the seismic hazard curve at the design site (the interval of integration adopted herein is from 0.005 g to 3.00 g). To this end, the SAC/FEMA closed-form probabilistic framework proposed by Cornell et al. [23] was adopted assuming a biased hazard fitting using a second-order power-law function as proposed by Vamvatsikos [24].

Fig. 15 shows a comparison of the annual PoE of different limit states, between the CFS-SWP and MRF structures. As far as the structures designed for Porto are concerned, the results are uniform in terms of trend, where the risk of exceeding any limit state is, as expected, lower for MRF than for CFS-SWP structures. This results from the higher lateral overstrength of the MRFs which is reflected in lower PoE of a given limit state in comparison to CFS-SWP structures. A similar conclusion has been drawn by previous researchers [25,53] based on a sensitivity study in which the lateral overstrength had a significant

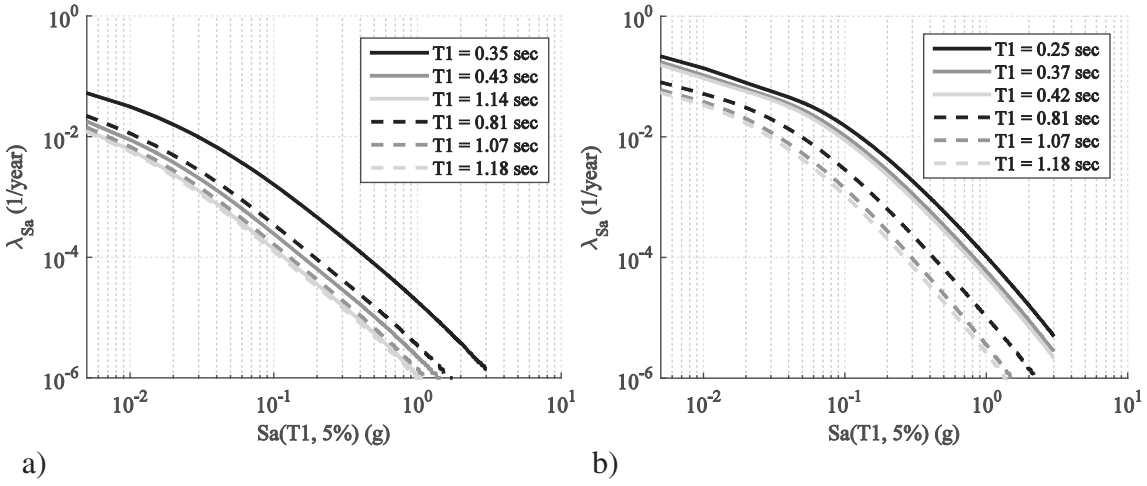

Fig. 14. Seismic hazard curves for: a) Porto and b) Lagos.

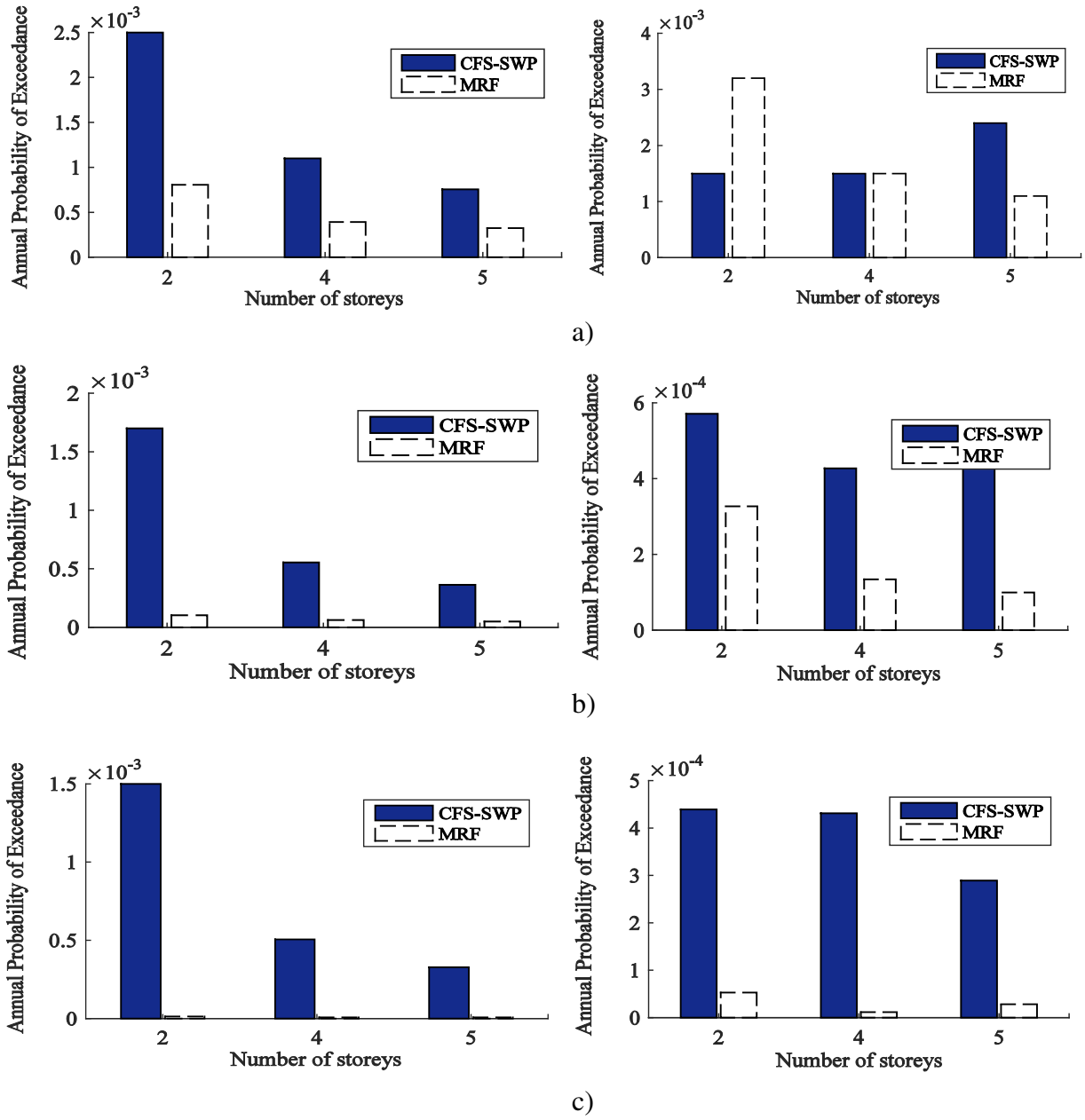

Fig. 15. Annual probability of exceeding: a) DL, b) NLC and c) NC limit states for regions of low (left) and moderate-to-high (right) seismicity. (Note: scales vary per limit state and region.)

effect on the fragility data. However, in the case of structures designed for Lagos, particularly the 2-storey building, the MRFs exhibited higher risk of exceeding the DL limit state in comparison to the CFS-SWP structures. This observation may be justified with the fact that the CFS-SWP structures have a lower fundamental period of vibration, and hence develop lower lateral deformation for the seismic intensity corresponding to the DL limit state. As illustrated in Fig. 16, the evaluation of the seismic risk, which involves the convolution of the PoE of the DL limit state and the hazard, results in a larger area for the 2-storey MRF in comparison to the CFS-SWP system. Disaggregation of the annual PoE of the DL limit state (Fig. 16) reveals that the lower half of the fragility curve contributed most to the annual PoE for the CFS structure. Conversely, for the MRF structure, the upper half of the fragility curve contributed most to the annual PoE. This observation stems from the lower standard deviation that characterizes the fragility curve of the MRF structure.

Disaggregation of the annual PoE of the NC limit state reveals that the intensities corresponding to the lower half of the fragility curve govern the amplitude of the annual PoE. The dominance of intensities lower than the median intensity is driven by the steep slope of the seismic hazard curve at these intensities (Fig. 14). Therefore, the Sa (T_1) levels that most contributed to the estimation of the annual PoE values are located towards the left tail of the fragility curve [54]. This is due to the fact that small magnitude earthquakes occur more frequently than large magnitude earthquakes. Therefore, when quantifying the annual PoE related to any limit state, it is more important to accurately estimate the left side of the fragility function, where the design Sa(T_1) level is located, than the right side of the function. This represents a good index to reduce uncertainty in the assessment of the annual PoE. Consequently, adopting a state-of-the-art characterization of the target response spectrum (the exact CMS) for the selection of ground motion records fits well with the above described criterion

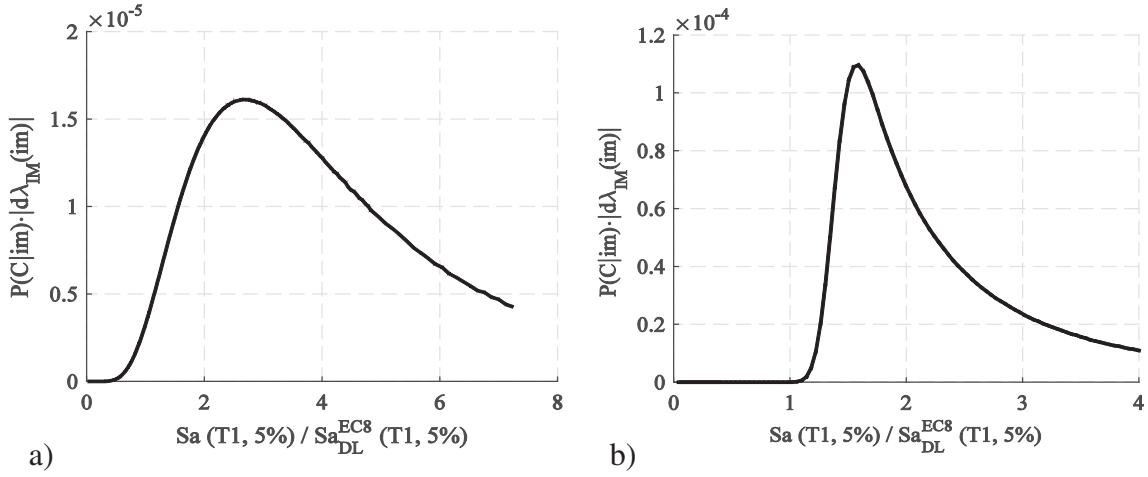

Fig. 16. λ_{DL} disaggregation curves of the 2-storey buildings located in Lagos: a) CFS-SWP and b) MRF.

since the absence of variability of $Sa(T_1)$ for all the selected ground motion records and the consistency with the seismic hazard of the site, for all relevant periods, is ensured. This is in line with the recommendation made by Lin et al. [55] where the CMS, for a risk-based assessment purpose, is considered as the most accurate target spectrum among UHS and CMS for the selection of ground motion records.

The annual PoE (risk) associated to the three limit states over the lifetime of the CFS-SWP and MRF structures are summarized in Table 6. Following the approach proposed by Pinto and Franchin [56] for extracting general limits of the annual probability of failure for different building classes and limit states, a simplified expression $2.25/T_R$ (where T_R is the return period), which is based on the hazard curve fitting, is adopted. Since the structures studied in this paper were designed for residential building occupancy, Class II buildings (ordinary) was considered which led to values of 4.5E−02, 4.7E−03 and 2.3E−03 for DL, NLC and NC limit states, respectively.

As illustrated in Table 6, all the structures considered in this study fulfil the prescribed limits. It is worth noting that the calculation of seismic risk is dependent on many factors and the associated uncertainty is substantial, where a small change in the hazard curve fitting could induce a significant increase or decrease on the seismic risk. Moreover, the approximation in the fit of the lognormal distribution that was adopted to derive the fragility curves also contributes to an uncertainty in the estimation of the seismic risk. This is deemed relevant, even when the parameters of the lognormal distribution are estimated using the Maximum Likelihood Fitting method [51]. Therefore, special care should be devoted to this source of uncertainty in risk-based assessment studies, as also referred in previous works [57,58]. Moreover, it is worth noting that, in this study, only the aleatory uncertainties have been taken into account through the consideration of the record-to-record variability. On the other hand, the epistemic uncertainties are knowledge-based and are most related to the physical properties of the structure and its modelling parameters. Since the level of knowledge in modelling the two types of structural systems is similar, the introduction of these uncertainties would affect the absolute value of the seismic risk, but would not have a significant impact on the relative comparison of the seismic performance of the two structural systems.

7. Summary and conclusions

The main objective of the research presented in this paper is the quantification of the seismic risk of the CFS-SWP adopting the more common conventional steel MRF as a benchmark system. Two-, 4- and 5-storey building of both structural systems have been designed for two different sites located in Portugal and for two seismic intensity levels. Seismic design was conducted based on the European seismic provisions, taking into consideration some recommendations previously proposed by the authors regarding the design of CFS-SWP systems for seismic resistance. The structures were modelled using the OpenSees software adopting novel deteriorating hysteresis models that are capable of reasonably capturing the structural response up to the onset of collapse. PSHA was conducted to characterize the seismic hazard. IDA was performed using site-specific ground motion records sets selected based on a realistic target response spectrum (CMS) derived from PSHA disaggregation data. For both structural system types, the annual

Table 6
Annual probability of the CFS-SWP and MRF structures exceeding different performance limit states.

Building	DL			NLC			NC		
	CFS-SWP	MRF	$\overline{\lambda_{DL}}$	CFS-SWP	MRF	$\overline{\lambda_{NLC}}$	CFS-SWP	MRF	$\overline{\lambda_{NC}}$
1	2.50E−3	8.06E−4	4.5E−2	1.70E−3	1.02E−4	4.7E−3	1.50E−3	1.34E−5	2.3E−3
2	1.10E−3	3.92E−4		5.54E−4	6.21E−5		5.06E−4	7.41E−6	
3	7.55E−4	3.24E−4		3.63E−4	4.96E−5		3.28E−4	7.92E−6	
4	1.50E−3	3.20E−3		5.71E−4	3.27E−4		4.39E−4	5.30E−5	
5	1.50E−3	1.50E−3		4.27E−4	1.34E−4		4.31E−4	1.17E−5	
6	2.40E−3	1.10E−3		4.35E−4	9.94E−5		2.89E−4	2.83E−5	

PoE for predefined limit states were determined. The main conclusions drawn from this study are listed as follows:

- The results showed the potential benefit of using lightweight cold-formed structural members to withstand lateral loads in low- and medium-rise buildings which favours the economical aspect without a significant cost in the structural performance.

- The values of the annual PoE shed light on the need for adopting a realistic target response spectrum for the selection of a ground motion record set. The obtained results reveal a non-negligible influence of the spectral shape of the ground motion records on the structural response, particularly for structural systems that have a deteriorating lateral behaviour and develop inelastic behaviour at low levels of deformation.

- The analyses conducted in this research showed that the probability of violating any limit state (DL, NLC and NC) falls within the prescribed limits. In general, MRFs are associated with lower levels of seismic risk. Nevertheless, the seismic risk associated to CFS-SWP system is still acceptable. Therefore, the latter can be considered as a reliable structural solution in achieving performance-based objectives for low- and medium-rise buildings located in low and moderate-to-high seismic areas.

Since non-structural components make up a considerable rate of the building's total construction cost, a more detailed comparison involving loss calculations of both structural and non-structural components is considered as a topic worthy of future research.

Acknowledgements

In the development of this research work, the support of Erasmus Mundus Battuta project through a PhD mobility scholarship (BT15DM2716), which has been awarded to the first author, is gratefully acknowledged.

References

[1] EN 1998-1, Eurocode 8, Design of Structures for Earthquake Resistance, Part 1: General Rules, Seismic Actions and Rules for Buildings, European Committee for Standardization, Brussels, CEN, 2005.
[2] A.E. Branston, C.Y. Chen, F.A. Boudreault, C.A. Rogers, Testing of light-gauge steel frame wood structural panel shear walls, Can. J. Civ. Eng. 33 (2006) 561–572, http://dx.doi.org/10.1139/106-014.
[3] C. Yu, Shear resistance of cold-formed steel framed shear walls with 0.686 mm, 0.762 mm, and 0.838 mm steel sheet sheathing, Eng. Struct. 32 (2010) 1522–1529http://dx.doi.org/10.1016/j.engstruct.2010.01.029.
[4] C. Yu, Y. Chen, Detailing recommendations for 1.83 m wide cold-formed steel shear walls with steel sheathing, J. Constr. Steel Res. 67 (2011) 97–101, http://dx.doi.org/10.1016/j.jcsr.2010.07.009.
[5] N. Balh, J. DaBreo, C. Ong-Tone, K. El-Saloussy, C. Yu, C.A. Rogers, Design of steel sheathed cold-formed steel framed shear walls, Thin-Walled Struct. 75 (2014) 76–86, http://dx.doi.org/10.1016/j.tws.2013.10.023.
[6] J. DaBreo, N. Balh, C. Ong-Tone, C.A. Rogers, Steel sheathed cold-formed steel framed shear walls subjected to lateral and gravity loading, Thin-Walled Struct. 74 (2014) 232–245, http://dx.doi.org/10.1016/j.tws.2013.10.006.
[7] P. Liu, K.D. Peterman, B.W. Schafer, Impact of construction details on OSB-sheathed cold-formed steel framed shear walls, J. Constr. Steel Res. 101 (2014) 114–123, http://dx.doi.org/10.1016/j.jcsr.2014.05.003.
[8] I. Shamim, J. DaBreo, C.A. Rogers, Dynamic testing of single-and double-story steel sheathed cold-formed steel framed shear walls, J. Struct. Eng. 139 (2013)http://dx.doi.org/10.1061/(ASCE)ST.1943-541X.0000594.
[9] R. Landolfo, L. Fiorino, G. Della Corte, Seismic behavior of sheathed cold-formed structures: physical tests, J. Struct. Eng. 132 (4) (2006) 570–581, http://dx.doi.org/10.1061/(ASCE)0733-9445(2006)132:4(570).
[10] O. Iuorio, L. Fiorino, R. Landolfo, Testing CFS structures: the new school BFS in Naples, Thin-Walled Struct. 84 (2014) 275–288, http://dx.doi.org/10.1016/j.tws.2014.06.006.
[11] L. Fiorino, O. Iuorio, V. Macillo, M.T. Terracciano, T. Pali, R. Landolfo, Seismic design method for CFS diagonal strap-braced stud walls: experimental validation, J. Struct. Eng. 142 (3) (2016)http://dx.doi.org/10.1061/(ASCE)ST.1943-541X.0001408.
[12] L. Fülöp, D. Dubina, Performance of wall-stud cold-formed shear panels under monotonic and cyclic loading part II: numerical modelling and performance analysis, Thin-Walled Struct. 42 (2) (2004) 339–349, http://dx.doi.org/10.1016/S0263-8231(03)00064-8.
[13] G. Della Corte, L. Fiorino, R. Landolfo, Seismic behavior of sheathed cold-formed structures: numerical study, J. Struct. Eng. 132 (4) (2006) 558–569, http://dx.doi.org/10.1061/(ASCE)0733-9445(2006)132:4(558).
[14] M. Vincenzo, O. Iuorio, M.T. Terracciano, L. Fiorino, R. Landolfo, Seismic response of CFS strap-braced stud walls: theoretical study, Thin-Walled Struct. 85 (2014) 301–312, http://dx.doi.org/10.1016/j.tws.2014.09.006.
[15] L. Fiorino, O. Iuorio, R. Landolfo, Sheathed cold-formed steel housing: a seismic design procedure, Thin-Walled Struct. 47 (8-9) (2009) 919–930, http://dx.doi.org/10.1016/j.tws.2009.02.004.
[16] R. Landolfo, L. Fiorino, O. Iuorio, A specific procedure for seismic design of cold-formed steel housing, Adv. Steel Constr. 6 (1) (2010) 603–618.
[17] L. Fiorino, O. Iuorio, V. Macillo, R. Landolfo, Performance based design of sheathed CFS buildings in seismic area, Thin-Walled Struct. 61 (2012) 248–257, http://dx.doi.org/10.1016/j.tws.2012.03.022.
[18] L. Fiorino, O. Iuorio, R. Landolfo, Designing CFS structures: the new school BFS in Naples, Thin-Walled Struct. 78 (2014) 37–47, http://dx.doi.org/10.1016/j.tws.2013.12.008.
[19] K.D. Peterman, Behavior of Full-Scale Cold-Formed Steel Buildings Under Seismic Excitations(PhD thesis) John Hopkins University, Baltimore, United States, 2014.
[20] J. Leng, Simulation of Cold-Formed Steel Structures(PhD thesis) John Hopkins University, Baltimore, United States, 2015.
[21] PEER, OpenSees: Open System for Earthquake Engineering Simulation, Pacific Earthquake Engineering Research Center, University of California, Berkeley, CA, 2006.
[22] J.W. Baker, Conditional mean spectrum: tool for ground-motion selection, J. Struct. Eng. 137 (3) (2011) 322–331, http://dx.doi.org/10.1061/(ASCE)ST.1943-541X.0000215.
[23] C.A. Cornell, F. Jalayer, R.O. Hamburger, D.A. Foutch, Probabilistic basis for 2000 SAC Federal Emergency Management Agency steel moment frame guidelines, J. Struct. Eng. 128 (4) (2002) 526–533, http://dx.doi.org/10.1061/(ASCE)0733-9445(2002)128:4(526).
[24] D. Vamvatsikos, Accurate application and second-order improvement of SAC/FEMA probabilistic formats for seismic performance assessment, J. Struct. Eng. 140 (2) (2014)http://dx.doi.org/10.1061/(ASCE)ST.1943-541X.0000774.
[25] S. Kechidi, N. Bourahla, J.M. Castro, Seismic design procedure for cold-formed steel shear wall frames: proposal and evaluation, J. Constr. Steel Res. 128 (2017) 219–232, http://dx.doi.org/10.1016/j.jcsr.2016.08.018.
[26] EN 1993-1-3, Eurocode 3, Design of Steel Structures, Part 1.3: General Rules for Cold Formed Thin Gauge Members and Sheeting, European Committee for Standardization, Brussels; CEN, 2007.
[27] AISI-S100, North American Specification for the Design of Cold-formed Steel Structural Members, American Iron and Steel Institute, Washington, D.C., 2016
[28] EN 1993-1-1, Eurocode 3: Design of Steel Structures - Part 1.1: General Rules and Rules for Buildings. European Committee for Standardization. Brussels: CEN, 2005.
[29] A.Y. Elghazouli, Assessment of European seismic design procedures for steel framed structures, Bulletin of Structural Engineering. 8 (2010) 65–89, http://dx.doi.org/10.1007/s10518-009-9125-6.
[30] J.M. Castro, F.J. Dávila-Arbona, A.Y. Elghazouli, Seismic design approaches for panel zones in steel moment frames, J. Earthq. Eng. 12 (S1) (2008) 34–51, http://dx.doi.org/10.1080/13632460801922712.
[31] AISI-S200, North American standard for cold-formed steel framing-general provisions, American Iron and Steel Institute, Washington, D.C, 2012.
[32] FEMA, Quantification of Building Seismic Performance Factors. FEMA P695, Federal Emergency Management Agency, Washington (DC), 2009.
[33] S. Kechidi, N. Bourahla, Deteriorating hysteresis model for cold-formed steel shear wall panel based on its physical and mechanical characteristics, Thin-Walled Struct. 98 (Part B) (2016) 421–430, http://dx.doi.org/10.1016/j.tws.2015.09.022.
[34] S. Kechidi, N. Bourahla, CFSWSWP uniaxialMaterial, http://opensees.berkeley.edu/wiki/index.php/CFSWSWP/ (accessed 31.07.2017).
[35] D.G. Lignos, H. Krawinkler, Deterioration modeling of steel components in support of collapse prediction of steel moment frames under earthquake loading, J. Struct. Eng. 137 (11) (2011) 1291–1302, http://dx.doi.org/10.1061/(ASCE)ST.1943-541X.0000376.
[36] M. Araújo, L. Macedo, J.M. Castro, Evaluation of the rotation capacity limits of steel members defined in EC8-3, J. Constr. Steel Res. 135 (2017) 11–29, http://dx.doi.org/10.1016/j.jcsr.2017.04.004.
[37] F. Zareian, D.G. Lignos, H. Krawinkler, Evaluation of seismic collapse performance of steel special moment resisting frames using FEMA P695 (ATC-63) methodology, Proceedings of Structures Congress ASCE, Orlando, Florida, May 12–14, 2010.
[38] H. Krawinkler, Shear in beam-column joints in seismic design of steel frames, Eng. J. 15 (3) (1978) 82–91.
[39] L. Macedo, Improved Performance-Based Seismic Design Methodologies for Steel Moment-Resisting Frames(PhD thesis) University of Porto, Portugal, 2017.
[40] L. Macedo, J.M. Castro, SelEQ: an advanced ground motion record selection and scaling framework, Adv. Eng. Softw. (2017)http://dx.doi.org/10.1016/j.advengsoft.2017.05.005.
[41] European Facility for Earthquake Hazard and Risk (EFEHR), available at: http://www.efehr.org:8080/jetspeed/portal/ (accessed 31.07.2017).
[42] S.P. Vilanova, J.F. Fonseca, Probabilistic seismic-hazard assessment for Portugal, Bull. Seismol. Soc. Am. 97 (5) (2007) 1702–1717, http://dx.doi.org/10.1785/0120050198.
[43] G.M. Atkinson, D.M. Boore, Earthquake ground-motion prediction equations for eastern North America, Bull. Seismol. Soc. Am. 96 (2006) 2181–2205, http://dx.doi.org/10.1785/0120050245.
[44] S. Akkar, J.J. Bommer, Empirical equations for the Prediction of PGA, PGV, and spectral accelerations in Europe, the Mediterranean Region, and the Middle East, Seismol. Res. Lett. 81 (2010) 195–206, http://dx.doi.org/10.1785/gssrl.81.2.195.
[45] V. Silva, Development of Open Models and Tools for Seismic Risk Assessment: Application to Portugal(PhD thesis) University of Aveiro, Portugal, 2013.
[46] T. Lin, S.C. Harmsen, J.W. Baker, N. Luco, Conditional spectrum computation incorporating multiple causal earthquakes and ground-motion prediction models, Bull. Seismol. Soc. Am. 103 (2A) (2013) 1103–1116, http://dx.doi.org/10.1785/0120110293.

[47] Pacific Earthquake Engineering Research Center (PEER), PEER NGA Database, University of California, Berkeley, CA, 2005 (http://peer.berkeley.edu/, accessed 31.07.2017).
[48] D. Vamvatsikos, C.A. Cornell, Incremental dynamic analysis, Earthq. Eng. Struct. Dyn. 31 (3) (2002) 491–514, http://dx.doi.org/10.1002/eqe.141.
[49] J.M. Martinez, Seismic Performance Assessment of Multi-Storey Buildings With Cold Formed Steel Shear Wall Systems(PhD thesis) University of Waterloo, Ontario, Canada, 2007.
[50] Seismic Evaluation and Retrofit of Existing Buildings (ASCE 41-13)2013 (555 p).
[51] J.W. Baker, Efficient analytical fragility function fitting using dynamic structural analysis, Earthquake Spectra 31 (1) (2015) 579–599, http://dx.doi.org/10.1193/021113EQS025M.
[52] C.B. Haselton, J.W. Baker, Ground motion intensity measures for collapse capacity prediction: choice of optimal spectral period and effect of spectral shape, 8th National Conference on Earthquake Engineering, April 18–22, 2006 (San Francisco, CA, United States).
[53] L.G. Vigh, G.G. Deierlein, E. Miranda, A.B. Liel, S. Tipping, Seismic performance assessment of steel corrugated shear wall system using nonlinear analysis, J. Constr. Steel Res. 85 (2013) 48–59, http://dx.doi.org/10.1016/j.jcsr.2013.02.008.
[54] L. Eads, E. Miranda, H. Krawinkler, D.G. Lignos, An efficient method for estimating the collapse risk of structures in seismic regions, Earthq. Eng. Struct. Dyn. 42 (1) (2013) 25–41, http://dx.doi.org/10.1002/eqe.2191.
[55] T. Lin, C.B. Haselton, J.W. Baker, Conditional spectrum-based ground motion selection. Part II: intensity-based assessments and evaluation of alternative target spectra, Earthq. Eng. Struct. Dyn. 42 (12) (2013) 1867–1884, http://dx.doi.org/10.1002/eqe.2303.
[56] P.E. Pinto, P. Franchin, Existing buildings: the new Italian provisions for probabilistic seismic assessment, Perspectives on European Earthquake Engineering and Seismology, Geotechnical, Geological and Earthquake Engineering, 34, 2014, pp. 97–130, http://dx.doi.org/10.1007/978-3-319-07118-3_3.
[57] B.A. Bradley, The seismic demand hazard and importance of the conditioning intensity measure, Earthq. Eng. Struct. Dyn. 41 (11) (2012) 1417–1437, http://dx.doi.org/10.1002/eqe.2221.
[58] M. Marques, L. Macedo, M. Araújo, L. Martins, J.M. Castro, L. Sousa, V. Silva, R. Delgado, Influence of Record Selection Procedures on Seismic Loss Estimations, Vulnerability, Uncertainty, and Risk, 2014 1756–1766, http://dx.doi.org/10.1061/9780784413609.176.